A Robust B-Splines-based Point Match Method for Non-rigid Surface Registration

Hesheng Wang [1] and Baowei Fei [2,1]
Departments of Biomedical Engineering[1] and Radiology[2]
Case Western Reserve University, Cleveland, OH, 44106

***Abstract*—Small animal imaging provides a powerful tool to study cancer in animal models. To monitor therapeutic response, serial *in vivo* images are acquired at different time points. Accurate image registration is needed to improve the quantification of changes over time. However, mouse body is extremely flexible and deformable, mouse image registration is challenging. In this paper, we present a deformable image registration method for the whole mouse body. A non-rigid point matching method has been developed to align mouse bones which represent the posture of a mouse body. Deformation is modeled as a global affine transformation followed by a local B-splines deformation. The robust point matching method simultaneously estimates point correspondence and surface deformation. It does not need to identify and label feature correspondences. The method can handle complex three-dimensional surfaces with a large amount of points and has achieved a high computational efficiency. The method was tested on mouse microCT images acquired at different positions. The distance between the anatomical feature point pairs has decreased from 3.8±1.0 mm for manually rigid-body registration to 0.9±0.4 mm for non-rigid surface registration. We also demonstrated the surface matching method for tumor magnetic resonance images that were acquired in different phases of treatment. The non-rigid surface registration method works well for both bone and soft tissues. The registration method can be applied to not only small animal images but also human images in clinical applications.**

Keywords; non-rigid image registration, small animal imaging, whole body registration, surface registration, b-splines, robust point matching

I. INTRODUCTION

Small animals including mice have been extensively used to study and model many human diseases [1]. Small animal imaging can screen the models and directly provide *in vivo* information of diseases processing and therapeutic effects. In order to follow up disease progression, quantify tumor growth and monitor biological response to therapies, images of mice at different time points or modalities need be aligned [2]. As a mouse body is quite small and very flexible, it is very difficult to maintain the mouse at the same position for each imaging session. The situation becomes more severe when considering mouse respiration and heart beating. Therefore, we are developing non-rigid image registration algorithms to match these images for improved quantification.

Intensity-based registration methods have a limited capture range [3] and typically require a rigid transformation to get two volumes roughly aligned at a preprocessing step. However, bones contain many articulated joints which cannot be modeled by a simply rigid transformation. Meanwhile, bone region in an image volume might not have enough intensity information for accurate intensity-based registration. Alternatively, feature-based surface registration could yield accurate results if the bone surfaces can be extracted from image volumes.

Although thin plate splines (TPS) based point matching method has shown promising for this application [4], the method can only work on surfaces that have a limited number of points. We are developing B-splines based point matching method for improved computation efficacy. We are also testing this surface matching method for tissue registration such as tumors.

II. METHOD

A. B-splines point-based surface matching

For a conventional point-based surface matching, two set of points X and V are sampled from both surfaces, and it is assumed that each point in X has a one-to-one corresponding point in V. The two corresponding point sets are denoted as x_a $(a=1, 2,...,N)$ and v_a $(a=1,2,..N)$ respectively. x_a or v_a represents the coordinate of point a in the volume, so it is a three element vector $\{x_{ax}, x_{ay}, x_{az}\}$.

We define T as the spatial transformation that deforms the point v_a to match the corresponding point x_a, and $T(v_a)$ gives the absolute position of the transformed v_a instead of the displacement. The transformation T consists of a global affine transformation and a local deformation.

$$T(v_a) = \theta v_a + d + T_{local}(v_a) \qquad (1)$$

θ is a 3×3 affine transformation matrix and d is a 3 elements translation vector. T_{local} is a local deformation to account for non-rigid shape variation between images.

A least square fitting method is employed to seek a spatial transformation T between point sets X and V by minimizing the following energy function:

$$E = \sum_{a=1}^{N} \left\| x_a - T(v_a) \right\|^2 + \beta \left\| LT \right\|^2 \qquad (2)$$

The first item is the Euclidan distance between each corresponding points so as to match the two sets; the second term is a smoothness constraint defined by the second order spatial derivatives of the transformation. Note that the global affine transformation (θ, d) is a linear function of pixel position, and the second spatial derivative is zero, so $\|LT\|^2 =$

$\|LT_{local}\|^2$. The global affine transformation can be easily solved using a standard least-square scheme.

A B-splines function is used to model the non-rigid local deformation. The function is defined by a control point grid Φ that is a uniformly lattice spaced with $n_x \times n_y \times n_z$ to cover the whole volume. The local deformation of point v_a can be written as a 3-D tensor product of cubic B-splines [5]

$$T_{local}(v_a) = \sum_{l=0}^{3}\sum_{m=0}^{3}\sum_{n=0}^{3} B_l(u)B_m(v)B_n(w)\phi_{i+l,j+m,k+n} \quad (3)$$

Where $i = \left[\frac{v_{ax}}{n_x}\right] - 1, j = \left[\frac{v_{ay}}{n_y}\right] - 1, k = \left[\frac{v_{az}}{n_z}\right] - 1$, $u = \frac{v_{ax}}{n_x} - \left[\frac{v_{ax}}{n_x}\right], v = \frac{v_{ay}}{n_y} - \left[\frac{v_{ay}}{n_y}\right], w = \frac{v_{az}}{n_z} - \left[\frac{v_{az}}{n_z}\right]$, ∅ is the b-splines parameter defined at the grid Φ, and B represents cubic B-splines basis function.

We used a fastest descent method to minimize the energy function in (2). The derivative of the transformation with respect to the control point at the position *(p, q, r)* is computed as

$$\frac{\partial T_{local}(v_a)}{\partial \phi_{p,q,r}} = B_l(u)B_m(v)B_n(w)\delta_{(p,q,r),(i+l,j+m,k+n)} \quad (4)$$

Here *i, j, k* follow the previous definition in B-splines deformation (3) and the derivative is nonzero only at the control point with position *p=i+l, q=j+m, r=k+n*. The spatial derivatives of each term in the smooth constraints have analogous tensor product shapes with $T(v_a)$.

B. Robust point matching for surface registration

In general, object surfaces are extracted by segmentation of 3D volumes, and then down sampled to get points sets in order to represent the surfaces. It is difficult if not impossible to extract exact corresponding points from two surfaces, and even cannot ensure point correspondence existence for some points. We incorporated the B-splines motion model into a robust point matching framework (TPS-RPM) [6]. The algorithm registered two point clouds by searching a thin plate splines (TPS) transformation without manually defined point correspondence. However, the method is limited by computational constraints from TPS whose transformation relates to all the points. So we modified the method by modeling the registration with an explicitly defined affine transformation and a local b-splines deformation.

For registering two point sets v_a *(a=1,2,...,N)* and x_i, *(i=1,2,...M)* with unknown points correspondence, the robust points matching method does not consider a point v_a is one-to-one corresponding to a point in *x*, but v_a is related to all the points in *x* with a ratio m_{ai} subjecting to $\sum_{a=1}^{N} m_{ai} = 1$ for *i=1,2,...M,* and $\sum_{i=1}^{M} m_{ai} = 1$ for *a=1,2,...,N.* In order to handle outlier situation, the corresponding ratio matrix $M = \{m_{ai}\}$ is added with one extra row and column in the end as the outliers, the extra entry will be given a non-zero value once a point is identified as outlier. If entries of Matrix *M* become either 1 or 0, the point-to-point correspondence is recovered. Thus, this method is a general version of the conventional point-based surface registration.

As the point correspondence is given by *M*, the registration is expected to minimize the point distance based on correspondence *M,* and the energy function becomes

$$E = \sum_{a=1}^{N}\sum_{i=1}^{M} m_{ai}\|x_i - T(v_a)\|^2 + \beta\|LT\|^2 + \alpha\|T_{local}(v_a)\|^2 + \lambda\|\theta - I\|^2 + \eta\sum_{a=1}^{N}\sum_{i=1}^{M} m_{ai}\log m_{ai} \quad (5)$$

Similar to Equation (2), the energy function first evaluates the point distance rated by m_{ai} and constrains the transformation smoothness on the second order spatial derivatives ($\|LT\|^2$). Because the algorithm iteratively estimates *M*, the point correspondence is far from true at initial stage. The global affine transformation should be limited by the distance from identity matrix *I* to avoid unphysical flipping or folding ($\|\theta - I\|^2$). Different from TPS-RPM method [4, 6], we found it is necessary to constrain the local b-splines deformation by ($\|T_{local}\|^2$) because a global affine transformation should be predominant when *M* is far from permutation matrix.

The entropy term $\sum_{a=1}^{N}\sum_{i=1}^{M} m_{ai} log m_{ai}$ enforces the positivity constraints of *M*. The matrix *M* is updated by computing the first derivatives of the energy equation (5),

$$m_{ai} = e^{-\frac{\|x_i - T(v_a)\|^2}{\eta}} \quad (6)$$

The constraints of *M* are satisfied by Sinkhorn's method which iterates row and column normalization of *M* [6]. Once *M* is computed, v_a is considered to correspond to a point $\sum_{t=1}^{T} m_{ta} x_t$. As the two point sets are one-to-one corresponded, the problem becomes a least-square fitting with b-splines deformation which is described in the previous section. Minimization of the energy function (5) becomes two interlocking optimizations: the estimation of correspondence matrix of *M* and a least square fitting for the transformation.

The parameter η specifies the degree of fuzziness of the corresponding matrix *M*. the matrix becomes more fuzzy as η increases; as η decreases, the correspondence matrix approaches a permutation matrix. The energy function is minimized in a determinant annealing schedule. Initial η (η_0) depends on the scale of the image size, we starts with η_0=0.5 and assumes the deformation is less than quarter of the image size, so the points' coordinates are scaled to [0, 2] at the beginning. Then η is linearly decreasing according to $\eta^{new} = 0.90 \cdot \eta^{old}$. The interlocking optimizations are repeated until convergence at each η. Final η^{final} is determined by the quality of extracting surface points, the better one-to-one correspondences the point sets have, the smaller η^{final} is desired. The algorithm repeats the annealing scheme for maximal times of 100 for our dataset according to the experiences.

The parameters β, α and λ balance between transformation constraints and surface matching. Matrix *M* is fuzzy at high η,

the transformation needs to be more rigid for global matching so that great parameters are expected; as η becomes smaller, a flexible non-rigid transformation is desired to register the two surfaces. The parameters are set to adaptively decrease following the annealing schedule.

III. RESULTS

In order to test the algorithm performance on recovering the transformation, we applied the method to 2D simulated data provided in [6]. Visually good point clouds matching were achieved for all 5 data pairs in both directions. A better registration was showed in Fig. 1c compared with the result (Fig. 1f) from TPS-RPM registration.

Our method was conducted on tumor MR images which were segmented from MR images acquired before, immediately after and 24 hours after a novel therapy called photodynamic therapy. The MR images were first registered using a rigid-body registration method [2]. Then, the tumors were segmented and the surfaces were aligned using the proposed method. Finally, the non-rigid surface transformation was applied to tumor MR images. Fig. 2 demonstrated the registration of tumor surfaces (Fig. 2d) and the overlap of the rendering surfaces (Fig. 2h). The overlap ratio between two segmented volumes has improved from 78 ± 3% after rigid registration to 91 ± 2% after the non-rigid registration for total 12 mouse experiments.

The method was applied to mouse microCT images which were acquired at three different positions using a microCT system. The images have a resolution of 0.1×0.1×0.1mm. We first manually aligned the volumes, then segmented the bones by a threshold (1200 unit), and finally down sampled the surfaces to get point lists (4800 ~ 5000 points). Our method succeeded in all experiments by visual inspection. The bones in Fig. 3b were registered to those in Fig. 3a. Fig. 3d showed the alignment of the bone surface after registration. We manually selected 5 anatomic feature point pairs from the two surfaces (Fig. 4a) and computed the distance between each point pair before and after registration. We also repeated the procedure of the manual registration, selection of feature point pairs for evaluation, and the surface registration for five times. Fig. 4b shows that the distance between the feature point pairs on the bones has improved from 3.8 ± 1.0 mm after manual registration to 0.9 ± 0.4 mm after the non-rigid registration.

IV. CONCLUSIONS

We developed a B-splines based non-rigid surface registration method to align the whole mouse body. A robust point matching method was developed to avoid identification of feature correspondence. We modeled the deformation with a global affine transformation followed by a local B-splines deformation, which made possible to explicitly constrain global and local transformation in the robust point matching framework. The local B-splines modeling and gradient based minimization enabled the method capable to handle complex surfaces with great amount of points with a high computation efficacy. The experiments show that the non-rigid surface matching method can effectively register tissue surfaces and bones. The method was applied to small animal images and it can be useful for clinical human images.

ACKNOWLEDGMENT

This work was partially supported by NIH grant R21CA120536 (PI: B Fei), by a Pilot Grant from the Case Comprehensive Cancer Center (PI: B Fei), and by Case Western Reserve University Presidential Research Initiative Award (PI: B Fei). The imaging facility is supported by the Northeastern Ohio Animal Imaging Resource Center as funded by NIH grant 5R24CA110943.

REFERENCES

[1] R.S.Balaban and V.A.Hampshire, "Challenges in small animal noninvasive imaging," ILAR J, vol. 42, pp. 248-262, 2001.

[2] B.Fei, H.Wang, R.F.Muzic, C.A.Flask, D.L.Wilson, J.L.Duerk, and N.L.Oleinick, "Deformable and rigid registration of microPET and high-resolution MR images for photodynamic therapy of cancer in mice," Medical Physics, vol. 23, pp. 753-760, 2006.

[3] D.L.Hill, P.G.Batchelor, M.Holden, and D.J.Hawkes, "Medical image registration," phys.Med.Biol, vol. 46, pp. R1-R45, 2001.

[4] X.Li, T.E.Peterson, J.C.Gore, and B.M.Dawant, "Automatic inter-subject registration of whole body images," WBIR 2006, LNCS 4057, pp. 18-25, 2006.

[5] D.Rueckert, L.I.Sonoda, C.Hayes, D.L.Hill, M.O.Leach, and D.J.Hawkes, "Nonrigid registration using free-form deformations: application to breast MR images," IEEE Trans Med Imaging, vol. 18, pp. 712-721, 1999.

[6] H.Chui and A.Ranagarajan, "A new point matching algorithm for non-rigid registration," Computer Vision and Image Understanding, pp. 114-141, 2003.

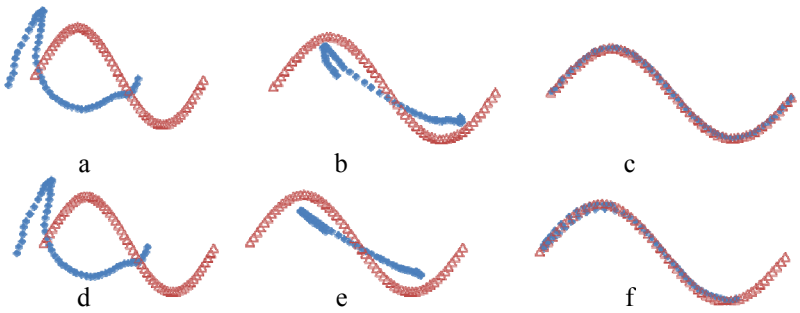

Figure 1. Registration of point sets in blue squares to point sets in red triangles. Registration resutls from the proposed method are shown in (a, b, c), (a) is the original point sets, (b) is a intermediate result and (c) is the final deformation of the point set. (d, e, f) are the registration results of TPS-RPM , (e) is a intermediate result and (f) is the final result indicating that portion of points were not registered.

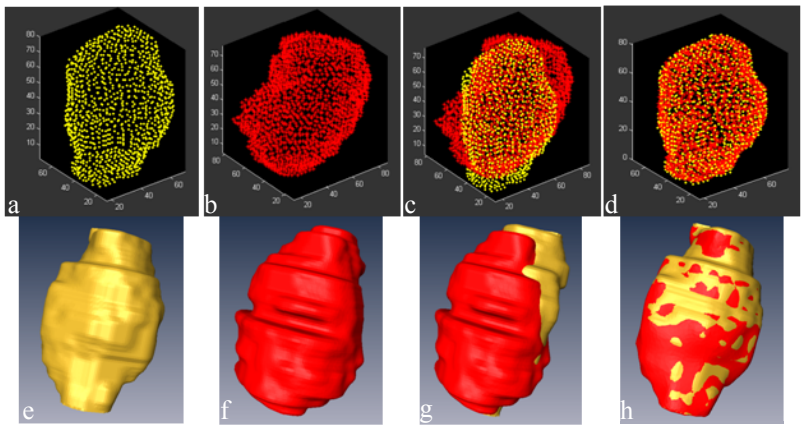

Figure 2. Surface registration of a tumor at different time points of treatment. (a) is the surface points of a tumor xenograft before treatment, and (b) is the surface points of the tumor 24h after the treatment, (c) is the overlap of the two point datasets. Surface points in (b) are deformed using the proposed method and (d) shows the color overlapping result after the non-rigid surface registration. The bottom row is the corresponding surface rendering for (a, b, c, d), respectively.

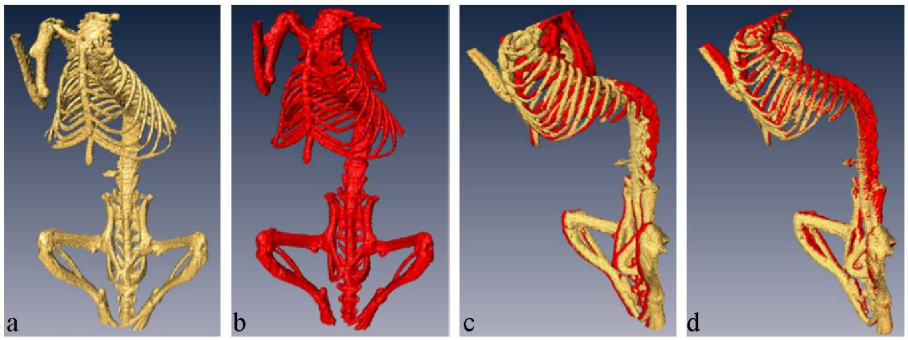

Figure 3. Surface registration for mouse bones in two different positions. (a) is the mouse bone from the reference volume, (b) is the bone from the floating volume, (c) is the overlap of the bone surfaces before registration, and (d) is the overlap of bone surfaces after the surface registration indicating better alignment of the bone structures.

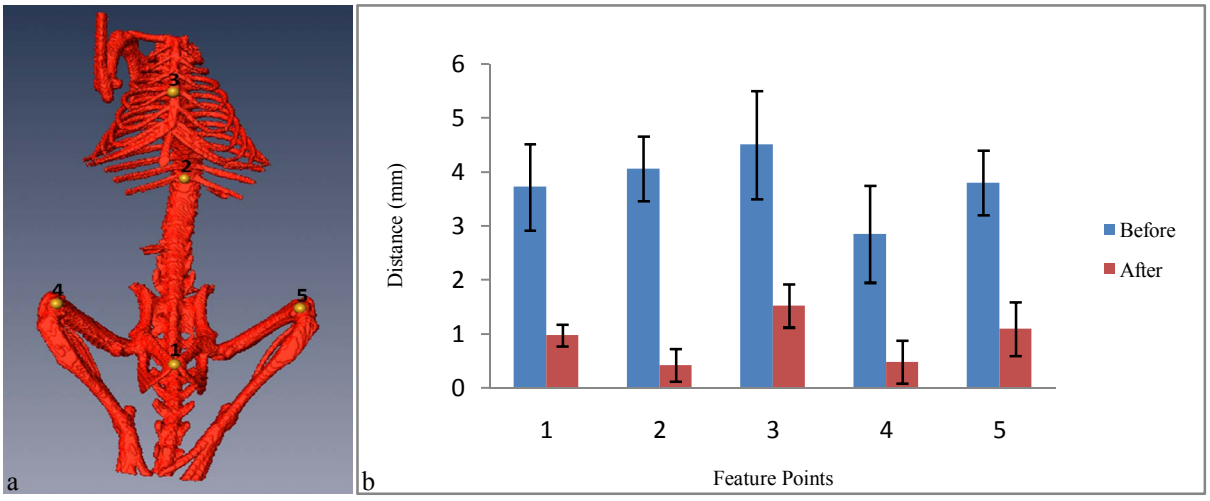

Figure 4. Distance of corresponding anatomic feature points before and after registration. (a) is the five manually selected anatomical feature points (1-5) on the both surfaces. The distances between corresponding points before and after registration were computed and compared in (b). The selection of feature points and the surface registration were repeated for five times. The error bars show the mean and standard deviation of the distance for each feature point. After the non-rigid surface registration, the bones are better registered.